

# Perfect quantum state transfer in a dispersion-engineered waveguide

Zeyu Kuang,<sup>1,\*</sup> Oliver Diekmann,<sup>1,\*</sup> Lorenz Fischer,<sup>1</sup> Stefan Rotter,<sup>1</sup> and Carlos Gonzalez-Ballesteros<sup>1,†</sup>

<sup>1</sup>*Institute for Theoretical Physics, TU Wien, Vienna A-1040, Austria*

(Dated: December 24, 2025)

High-fidelity state transfer is fundamentally limited by time-reversal symmetry: one qubit emits a photon with a certain temporal pulse shape, whereas a second qubit requires the time-reversed pulse shape to efficiently absorb this photon. This limit is often overcome by introducing active elements. Here, we propose an alternative solution: by tailoring the dispersion relation of a waveguide, the photon pulse emitted by one qubit is passively reshaped into its time-reversed counterpart, thus enabling perfect absorption. We analytically derive the optimal dispersion relations in the limit of small and large qubit-qubit separations, and numerically extend our results to arbitrary separations via multiparameter optimization. We further propose a spatially inhomogeneous waveguide that renders the state transfer robust to variations in qubit separations. In all cases, we obtain near-unity transfer fidelity ( $\geq 98\%$ ). Our dispersion-engineered waveguide provides a compact and passive route toward on-chip quantum networks, highlighting engineered dispersion as a powerful resource in waveguide quantum electrodynamics.

Quantum networks are key platforms for quantum communication [1–3], distributed computation [4–6], and fundamental studies of many-body physics [7–11]. They rely on the faithful transfer of quantum states between distant nodes [12–15]. Among many possible realizations, waveguide quantum electrodynamics (QED) provides a particularly natural setting [16–18], as waveguides can efficiently channel photons between spatially separated qubits. Yet even in the ideal case of two identical qubits coupled to a perfectly chiral waveguide [18–20], where every photon emitted by the first qubit is guided toward the second [Fig. 1(a)], perfect transfer is limited by a fundamental mismatch: the first qubit emits a photon with a certain temporal pulse shape, whereas the second qubit requires a time-reversed pulse shape to absorb the photon efficiently [21–23]. In the Markovian limit, this pulse asymmetry limits the excited-state occupation of the second qubit to a maximum of  $4/e^2 \approx 0.54$  [21], regardless of the group velocity, distance, or qubit-waveguide coupling rate.

A wide range of solutions have been proposed to overcome this state transfer limitation. The seminal work of Cirac *et al.* [12] introduces an external laser to dynamically tune the effective qubit-waveguide coupling rates, thereby forcing the emission of a time-reversal-symmetric pulse. This idea has been demonstrated experimentally [14, 24, 25] and extended theoretically to account for pulse distortions [26], dissimilar atoms [27], and multiplexed state transfer [28]. The principle of this active control can be generalized by replacing the external driving laser by other active elements such as a tunable cavity [26, 29], an intermediate atom with tunable coupling rate [30], or an atom ensemble [31]. A potential alternative route, which remains unexplored for quantum state transfer, is to modulate the waveguide to time-reverse the propagating pulse via a time-lens [32–34]. The general principle behind these diverse approaches is that they all use active, time-dependent modulation to

time-reverse the pulse and therefore achieve perfect state transfer. While versatile, these active components require additional monitor and control, making the overall system more complex.

In this Letter, we propose a passive method for perfect

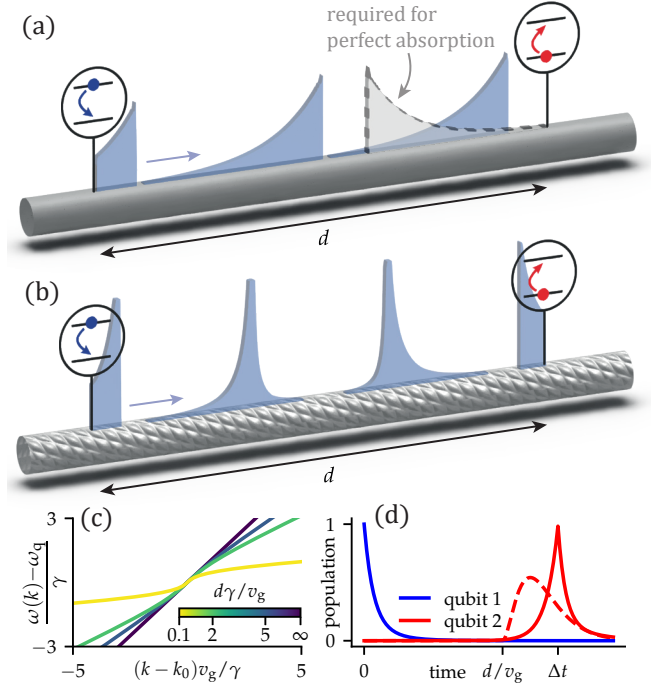


FIG. 1. State transfer between two qubits coupled to a chiral waveguide with (a) linear and (b) engineered dispersions. Snapshots of the emitted photon pulse are shown at different times. (c) Dispersion relations required for perfect state transfer (see text for details) for different qubit-qubit distances  $d$  (normalized by the pulse width  $v_g/\gamma$ ). (d) Qubit population dynamics in the dispersion-engineered waveguide (solid lines) and the linear-dispersion waveguide (dashed red line for the second qubit).

quantum state transfer, namely to engineer the *dispersion relation* of the waveguide. The resulting dispersion-engineered waveguide time-reverses the emitted pulse [see Fig. 1(b)] by providing the necessary phase shift at each frequency. Based solely on linear and passive photonics, our waveguide can be potentially realized using standard techniques in integrated photonics [17, 35, 36]. It suggests new opportunities of photonic design in quantum optics [37–39] and highlights engineered, dispersive few-photon pulse propagation as a potential powerful asset in waveguide QED.

We consider the system shown in Fig. 1(a): two identical qubits, located at positions  $x_1 = 0$  and  $x_2 = d$ , chirally coupled to a single-band, one-dimensional electromagnetic waveguide. In the rotating-wave approximation, the Hamiltonian reads ( $\hbar = 1$ )

$$H = \sum_{i=1}^2 \omega_q \sigma_i^+ \sigma_i^- + \int_0^\infty dk \omega(k) a_k^\dagger a_k + \sum_{i=1}^2 \int_0^\infty dk [e^{ikx_i} g(k) a_k \sigma_i^+ + \text{H.c.}], \quad (1)$$

where  $\omega_q$  is the qubit transition frequency,  $a_k$  is the annihilation operator for right-propagating photons of wave number  $k$  and frequency  $\omega(k)$ , and  $\sigma_i^\pm$  are the raising and lowering operators of qubit  $i$ . We assume the coupling is perfectly chiral [40–42] (i.e., the qubits only couple to right-propagating photons) and spectrally flat around  $\omega_q$ , such that we can approximate  $g(k) = g \theta(k)$  with the Heaviside function  $\theta(k)$ . The system wavefunction in the single-excitation subspace is

$$|\psi(t)\rangle = \left( \sum_{i=1}^2 c_i(t) \sigma_i^+ + \int_0^\infty dk c(k; t) a_k^\dagger \right) |g_1 g_2, 0\rangle, \quad (2)$$

where  $|g_i\rangle$  denotes the ground state of qubit  $i$ ,  $|0\rangle$  the vacuum of the waveguide field, and  $c_i(t)$  and  $c(k; t)$  the corresponding amplitudes. We aim at maximizing  $|c_2(t)|$  for an initial state where the first qubit is excited at  $t = 0$  while the second qubit and the field are in their ground states, i.e.,  $c_1(0) = 1$  and  $c_2(0) = c(k; 0) = 0$ .

Our hypothesis that a nonlinear dispersion  $\omega(k)$  can enable perfect quantum-state transfer is most transparent in the perturbative limit, where deviations from a linear dispersion are small. In this limit, we can use the Markovian Wigner–Weisskopf theory of spontaneous emission [43, 44] to represent the photon emitted by the first qubit at time  $t = 0$  classically as an electric field with an exponentially decaying envelope:  $E(x_1, t) = \theta(t) e^{-(\gamma + i\omega_q)t}$  where the decay rate  $\gamma = \pi g^2/v_g$  is governed by the coupling strength  $g$  and on-resonance group velocity  $v_g = (d\omega/dk)|_{\omega=\omega_q}$ . Its frequency spectrum is  $E(x_1, \omega) = 1/[\gamma - i(\omega - \omega_q)]$ . After propagating through a waveguide with an arbitrary single-band dispersion  $k(\omega)$ , the field at the position of the second qubit becomes  $E(x_2, \omega) = E(x_1, \omega) e^{ik(\omega)d}$ . For perfect absorption

at some time  $t = \Delta t$ , the second qubit must receive a field whose envelope is the *time-reverse* of the emitted field [21], i.e.,  $E_{\text{target}}(x_2, t) = \theta(\Delta t - t) e^{(\gamma - i\omega_q)(t - \Delta t)}$  or, in frequency domain,  $E_{\text{target}}(x_2, \omega) = e^{i\omega\Delta t}/[\gamma + i(\omega - \omega_q)]$ . Equating  $E(x_2, \omega) = E_{\text{target}}(x_2, \omega)$ , we obtain the required dispersion relation

$$k(\omega) = \frac{\Delta t}{d} \omega - \frac{2}{d} \arctan\left(\frac{\omega - \omega_q}{\gamma}\right). \quad (3)$$

The transfer time  $\Delta t$  can be determined by combining Eq. (3) with the definitions of  $v_g$  and  $\gamma$ , yielding  $\Delta t = d/v_g + 2/\gamma$ . Equation (3) is the key dispersion that converts an exponentially decaying pulse at the position of the first qubit into its time-reversed, exponentially rising counterpart at the position of the second. This conversion process is illustrated in Fig. 1(b).

Figure 1(c) shows the dispersion of Eq. (3) for several qubit-qubit separations  $d$  (here we take  $\gamma = \pi \times 10^{-4} \omega_q$ ). Note that the group velocity  $d\omega/dk$  peaks near the resonance frequency  $\omega_q$ , indicating that near-resonant components travel faster than off-resonant ones. This behavior is precisely what the time-reversal conversion in Fig. 1(b) requires: to transform a decaying pulse into a rising one, the slowly varying tail of the exponential envelope (dominated by near-resonant frequencies) must overtake its rapidly varying front (where off-resonant frequencies reside). As the separation  $d$  increases, the required difference in group velocity decreases, since the tail has more time to overtake the front; consequently, the dispersion becomes increasingly linear, as seen in Fig. 1(c). In this regime the dispersion is consistent with our perturbative assumption, implying that for sufficiently large  $d$ , the analytical dispersion of Eq. (3) should result in perfect state transfer. This is demonstrated in Fig. 1(d) where already for  $d = 5v_g/\gamma$  (five pulse widths), the dispersion of Eq. (3) results in a 98% excitation probability of the second qubit (solid line) at the transfer time  $\Delta t$ , far above the 54% maximum attainable with a linear dispersion (dashed line). At larger distances the excitation probability asymptotically approaches 100%. These excitation probabilities are obtained by exact diagonalization of the Hamiltonian in Eq. (1) within the single-excitation subspace.

Although the dispersion of Eq. (3) enables near-perfect state transfer for qubits that are far apart, it fails when the qubits are brought close together. This can be seen in Fig. 2(a) where the maximum excitation probability of the second qubit (orange curve), calculated using the dispersion of Eq. (3), drops rapidly as the qubit distance  $d$  decreases. The origin is evident in Fig. 1(c): when the distance  $d$  becomes comparable to  $v_g/\gamma$  (the pulse width), the required dispersion becomes highly nonlinear. In this regime, the Markovian approximation no longer holds, and the qubit no longer decays exponentially, so that its emitted photon no longer has an exponential pulse envelope. Consequently, the phase compensation prescribed by Eq. (3) becomes inaccurate, and perfect

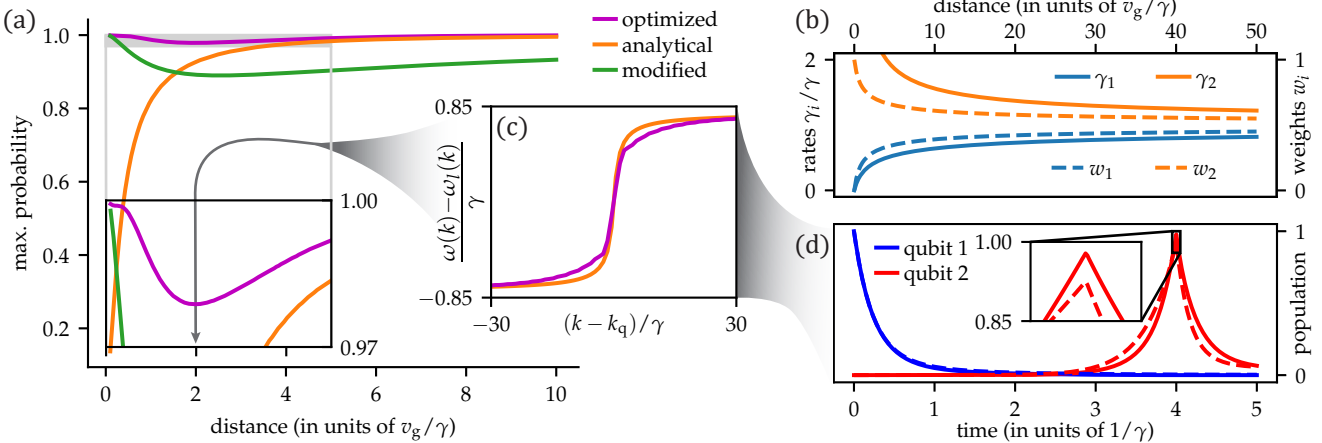


FIG. 2. (a) Maximum absorption probability of the second qubit using the analytical [orange, see Eq.(3)], small-distance [green, see Eq. (5)] and numerically optimized [purple] dispersion relations. As before, we assume  $\gamma = \pi \times 10^{-4} \omega_q$ . In the small-distance limit, the first qubit decays biexponentially under the analytical dispersion of Eq. (3). The decay rates and weights [defined in Eq. (4)] are plotted against the qubit distance  $d$  in (b). (c) Dispersion relation at  $d = 2v_g/\gamma$  where the linear contribution  $\omega_l \equiv \omega \Delta t/d$  has been subtracted for better visualization. (d) Populations as a function of time for the dispersion relations of panel (c). The dashed lines are for the analytical dispersion; the solid lines are for the numerically optimized dispersion.

state transfer is lost.

To overcome this challenge in the small- $d$  regime, we refine our previously derived dispersion through an iterative procedure. In our previous derivation, we have assumed a nearly linear dispersion to obtain an exponential emission profile, and used it to derive the dispersion of Eq. (3). We now take this dispersion as input to *update* the emission profile and, from it, construct a refined dispersion. As the new “input dispersion” of Eq. (3) is now nonlinear, Wigner–Weisskopf theory cannot be applied. We instead analytically and exactly compute the full qubit dynamics using the resolvent method (see End Matter). The resulting excitation amplitude of the first qubit is

$$c_1(t) = w_1 e^{-(i\omega_q + \gamma_1)t} - w_2 e^{-(i\omega_q + \gamma_2)t}, \quad (4)$$

where  $\gamma_1 = \xi - \sqrt{\xi^2 - \gamma^2}$ ,  $\gamma_2 = \xi + \sqrt{\xi^2 - \gamma^2}$ ,  $\xi = \gamma + v_g/d$ , and  $w_i = (\gamma_i - \gamma)/(\gamma_1 - \gamma_2)$ . Its decay is thus no longer exponential but *bi*-exponential. Figure 2(b) shows how the two decay rates  $\gamma_{1,2}$  and their weights  $w_{1,2}$  depend on the qubit distance  $d$ : for  $d \gg v_g/\gamma$ , both decay rates approach the Markovian value:  $\gamma_{1,2} \rightarrow \gamma$ , recovering the single-exponential decay. For smaller  $d$ , the two rates become different, explaining why the dispersion of Eq. (3) fails to yield perfect transfer for small  $d$ : the dispersion is designed to invert a single exponential pulse, yet the emitted pulse under this dispersion is biexponential and therefore not perfectly inverted. We continue our iterative procedure by computing the photon amplitudes  $c_k(t)$  analytically, and use them to extract a new optimal dispersion relation  $\omega(k)$ . Unfortunately, we find there is no single-band solution for the dispersion relation (see End Matter). However, we can harness that fact that, as evidenced by Fig. 2(b), for sufficiently small separations

( $d \ll v_g/\gamma$ ), the biexponential weights tend to  $w_1 \rightarrow 0$  and  $w_2 \rightarrow -1$ , so that the emission of qubit 1 becomes again dominated by a single exponential with modified decay rate  $\gamma_2$ . This indicates that in this limit, the dispersion of Eq. (3), which is designed to optimally invert an exponentially decaying pulse, should also lead to perfect absorption under the substitution of the Markovian decay rate  $\gamma$  by the modified rate  $\gamma_2$ , i.e.,

$$k_{d \rightarrow 0}(\omega) = \frac{\Delta t}{d} \omega - \frac{2}{d} \arctan\left(\frac{\omega - \omega_q}{\gamma_2}\right). \quad (5)$$

The maximum qubit occupation corresponding to this dispersion is shown by the green curve in Fig. 2(a). As expected, this dispersion successfully restores perfect quantum state transfer in the  $d \ll v_g/\gamma$  limit, precisely where the original dispersion of Eq. (3) fails (orange curve). Remarkably, by choosing one of our two analytical expressions in the large- $d$  and small- $d$  limit, state transfer with probability  $> 90\%$  can be achieved for any separation  $d$ .

To increase the fidelity beyond that achieved by the analytical dispersions of Eqs. (3) and (5), we perform a systematic multiparameter numerical optimization of the dispersion relation. For each qubit separation  $d$ , we initialize the optimization with the analytical dispersion of Eq.(3) and allow its shape to vary freely in order to maximize the excitation probability of the second qubit,  $|c_2(\Delta t, \omega(k))|^2$ . Both the dispersion curve  $\omega(k)$  and the transfer time  $\Delta t$  (this time is not known *a priori*) are our optimization variables. We parameterize  $\omega(k)$  on a finite frequency grid (roughly 2000 points) centered around  $\omega_q$  and evaluate the resulting two-qubit dynamics by exact diagonalization at each iteration. The gradient of the objective function  $|c_2(\Delta t, \omega(k))|^2$  with respect to  $\omega(k)$  and  $t$

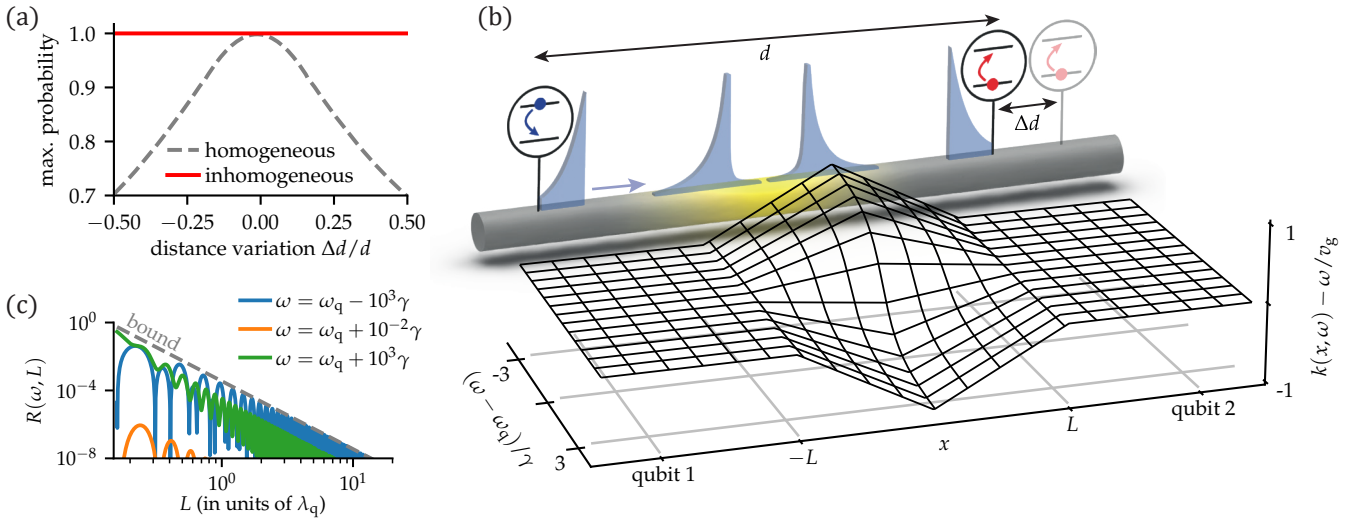


FIG. 3. (a) Maximal excitation probability of the second qubit (dashed gray line) versus deviation  $\Delta d$  from the assumed separation  $d$  [see (b) for an illustration]. The state transfer fidelity decreases with  $|\Delta d|$ . We propose to solve this by a spatially inhomogeneous waveguide, whose dispersion (minus the linear part, for visibility) is shown by the 3D mesh grid in (b). This dispersion varies adiabatically in space within a length  $2L$ , minimizing reflection and effectively suppressing it for  $L \gtrsim \lambda_q \equiv 2\pi v_g/\omega_q$  (panel c). The dispersion of this segment is chosen to time-reverse the pulse. As a result, the maximum occupation of qubit 2 is near unity regardless of the distance variation [(a), red line].

is obtained via the adjoint method [45–47] (see End Matter). The performance of the obtained optimized dispersion is shown by a purple curve in Fig. 2(a), and recovers the analytical limits at large and small  $d$ . This dispersion markedly improves transfer fidelity in the intermediate separation regime; the largest gains occur near  $d \approx 2v_g/\gamma$ , where the optimized dispersion [purple line in Fig. 2(c)] increases the second-qubit excitation probability from 92% to 98% [Fig. 2(d)]. Note that the optimized dispersion does still not achieve unit transfer fidelity, with a residual infidelity that becomes maximal ( $\sim 2\%$ ) at  $d = 2v_g/\gamma$ . This may stem from our restricted parameter search [currently restricted to dispersions close to Eq. (3)] or it may reflect a fundamental limitation of dispersion engineering when only a single band is available. In practice, this limitation can be bypassed by tuning the coupling strength  $g$ . Indeed, due to the scale invariance of the dynamics under the transformation  $d \rightarrow d/s$ ,  $g \rightarrow g/\sqrt{s}$ ,  $\omega(k) \rightarrow \omega(k/s)$  for any  $s \neq 0$ , one can always map the system into a regime where perfect transfer is achievable.

So far, all our proposed dispersions (either analytically derived or computationally optimized) are optimized for a given fixed qubit-qubit separation  $d$ . As a consequence, their performance for state transfer degrades when qubit 2 is imperfectly positioned at a distance  $d + \Delta d$  [illustrated in Fig. 3(b)]. This is shown by the dashed gray line in Fig. 3(a), which corresponds to the occupation of qubit 2 as a function of  $\Delta d$ , for  $d = 15v_g/\gamma$  and  $\gamma = \pi \times 10^{-4}\omega_q$ . Although the state transfer is still better than in linear-dispersion waveguides, the fidelity is far from 100% for significant deviations  $\Delta d$ , decreasing below  $\sim 90\%$  for

$\Delta d = d/4$  and below 70% for  $\Delta d = d/2$ . We find very similar values for the deterioration of fidelity for other values of  $d$ . The physical reason behind this deterioration is that the dispersion relation is chosen to perfectly time-reverse the pulse at a distance  $d$  from qubit 1. Since the dispersion is nonlinear, propagation by an extra distance  $\Delta d$  distorts the pulse into a shape that is not optimally absorbed by the second qubit. The further the extra distance  $\Delta d$ , the more the pulse shape will distort, and the worse the excitation of qubit 2 will be.

We solve this problem by placing the two qubits on two *dispersionless* sections of the waveguide and only engineer the dispersion in between. This new architecture is illustrated in Fig. 3(b) with the dispersionless region marked by gray and the dispersive region by yellow. The two qubits can be placed anywhere in the dispersionless region, and the pulse emitted by the first qubit will always decay exponentially and propagate toward the dispersive region without distortion. The dispersive region occupies a length  $2L$  and is dispersion-engineered to provide a frequency-dependent phase shift  $\Delta\phi(\omega) = -2\arctan[(\omega - \omega_q)/\gamma]$ , which converts the exponentially decaying pulse to an exponentially rising one [see Eq. (3)]. More specifically, this phase shift is implemented through a spatially inhomogeneous dispersion profile,  $k(\omega, x) = \omega/v_g + W(x)\Delta\phi(\omega)(1 - |x|/L)/L$ , where  $v_g$  denotes the group velocity in the dispersionless regions, and  $W(x) = \theta(x+L) - \theta(x-L)$  is a window function with  $\theta(x)$  the Heaviside function. The nonlinear part of this dispersion, illustrated in Fig. 3(b), gives exactly the required total phase shift:  $\int_{-L}^L [k(x, \omega) - \omega/v_g] dx = \Delta\phi(\omega)$ .

The spatial variation of the dispersion must be adiabatic to avoid unwanted reflections. Our analytical calculation (see End Matter) shows that in the large- $L$  limit, the reflection is bounded by  $R(\omega) \leq [\lambda/(2\pi L)]^4$ , where  $\lambda = 2\pi v_g/\omega$  is the wavelength of light in the dispersionless region. This is shown in Fig. 3(c), where both on- and off-resonant frequencies decay rapidly for large  $L$  according to the bound. The resulting inhomogeneous waveguide can be described by a Hamiltonian similar to Eq. (1), and its dynamics is solved by exact diagonalization (see End Matter). As shown by the red line in Fig. 3(a), with  $L = 3v_g/\gamma$ , the excitation probability of the second qubit reaches perfect fidelity for all qubit separations, in stark contrast to the homogeneous dispersion case, which is optimal for only one specific distance. Our inhomogeneous design shows that by leveraging the additional spatial degrees of freedom in the dispersion, we can provide full robustness of state-transfer against distance variations of the qubits.

In summary, we propose a route to perfect single-photon state transfer in waveguide QED by engineering the dispersion of the waveguide. We analytically derive the required dispersion for qubits that are far apart [Eq. (3)] and close-together [Eq. (5)], and numerically optimize it for regions in between. We also propose a new waveguide architecture that preserves perfect transfer even when the qubit positions are not correctly determined or later reconfigured. Our approach is fully passive during propagation and can be directly extended to design quantum memories by using standard  $\Lambda$ -type capture schemes [16, 48, 49]. Our proposed dispersion could be realized in existing photonic waveguides [50–54] or coupled-oscillator/spin-chain platforms [55–59], potentially further optimized via inverse designs [60–62]. Looking forward, this approach could be generalized to the transfer of multi-excitation states between emitter ensembles [9, 63–65], such as entangled [66, 67] or collective superradiant states [68–70].

This research was funded in part by the Austrian Science Fund (FWF) [10.55776/PAT1177623], [10.55776/COE1] and the European Union – NextGenerationEU. The computational results have been achieved using the Austrian Scientific Computing (ASC) infrastructure. We thank Carmen Buchegger for useful discussions.

\* These authors contributed equally to this work.  
 † carlos.gonzalez-ballesteros@tuwien.ac.at

[1] S. L. Braunstein and H. J. Kimble, Teleportation of Continuous Quantum Variables, *Phys. Rev. Lett.* **80**, 869 (1998).  
 [2] A. Furusawa, J. L. Sørensen, S. L. Braunstein, C. A. Fuchs, H. J. Kimble, and E. S. Polzik, Unconditional Quantum Teleportation, *Science* **282**, 706 (1998).  
 [3] H. Zheng and H. U. Baranger, Persistent Quantum Beats and Long-Distance Entanglement from Waveguide-Mediated Interactions, *Phys. Rev. Lett.* **110**, 113601 (2013).  
 [4] D. E. Chang, A. S. Sørensen, E. A. Demler, and M. D. Lukin, A single-photon transistor using nanoscale surface plasmons, *Nature Phys* **3**, 807 (2007).  
 [5] H. Zheng, D. J. Gauthier, and H. U. Baranger, Waveguide-QED-Based Photonic Quantum Computation, *Phys. Rev. Lett.* **111**, 090502 (2013).  
 [6] S. Mahmoodian, P. Lodahl, and A. S. Sørensen, Quantum Networks with Chiral-Light–Matter Interaction in Waveguides, *Phys. Rev. Lett.* **117**, 240501 (2016).  
 [7] D. E. Chang, V. Gritsev, G. Morigi, V. Vuletić, M. D. Lukin, and E. A. Demler, Crystallization of strongly interacting photons in a nonlinear optical fibre, *Nature Phys* **4**, 884 (2008).  
 [8] H. Zheng, D. J. Gauthier, and H. U. Baranger, Waveguide QED: Many-body bound-state effects in coherent and Fock-state scattering from a two-level system, *Phys. Rev. A* **82**, 063816 (2010).  
 [9] S. Mahmoodian, G. Calajó, D. E. Chang, K. Hammerer, and A. S. Sørensen, Dynamics of Many-Body Photon Bound States in Chiral Waveguide QED, *Phys. Rev. X* **10**, 031011 (2020).  
 [10] T. Armon, S. Ashkenazi, G. García-Moreno, A. González-Tudela, and E. Zohar, Photon-Mediated Stroboscopic Quantum Simulation of a Z-2 Lattice Gauge Theory, *Phys. Rev. Lett.* **127**, 250501 (2021).  
 [11] C. Tabares, A. Muñoz de las Heras, L. Tagliacozzo, D. Porras, and A. González-Tudela, Variational Quantum Simulators Based on Waveguide QED, *Phys. Rev. Lett.* **131**, 073602 (2023).  
 [12] J. I. Cirac, P. Zoller, H. J. Kimble, and H. Mabuchi, Quantum State Transfer and Entanglement Distribution among Distant Nodes in a Quantum Network, *Phys. Rev. Lett.* **78**, 3221 (1997).  
 [13] H. J. Kimble, The quantum internet, *Nature* **453**, 1023 (2008).  
 [14] T. E. Northup and R. Blatt, Quantum information transfer using photons, *Nature Photon* **8**, 356 (2014).  
 [15] A. Blais, A. L. Grimsmo, S. Girvin, and A. Wallraff, Circuit quantum electrodynamics, *Rev. Mod. Phys.* **93**, 025005 (2021).  
 [16] A. S. Sheremet, M. I. Petrov, I. V. Iorsh, A. V. Poshakinskiy, and A. N. Poddubny, Waveguide quantum electrodynamics: Collective radiance and photon-photon correlations, *Rev. Mod. Phys.* **95**, 015002 (2023).  
 [17] A. González-Tudela, A. Reiserer, J. J. García-Ripoll, and F. J. García-Vidal, Light–matter interactions in quantum nanophotonic devices, *Nat Rev Phys* **6**, 166 (2024).  
 [18] P. Lodahl, S. Mahmoodian, S. Stobbe, A. Rauschenbeutel, P. Schneeweiss, J. Volz, H. Pichler, and P. Zoller, Chiral quantum optics, *Nature* **541**, 473 (2017).  
 [19] D. De Bernardis, Z.-P. Cian, I. Carusotto, M. Hafezi, and P. Rabl, Light-Matter Interactions in Synthetic Magnetic Fields: Landau-Photon Polaritons, *Phys. Rev. Lett.* **126**, 103603 (2021).  
 [20] D. De Bernardis, F. S. Piccioli, P. Rabl, and I. Carusotto, Chiral Quantum Optics in the Bulk of Photonic Quantum Hall Systems, *PRX Quantum* **4**, 030306 (2023).  
 [21] M. Stobińska, G. Alber, and G. Leuchs, Perfect excitation of a matter qubit by a single photon in free space, *EPL* **86**, 14007 (2009).  
 [22] G. Leuchs and M. Sondermann, Time-reversal symmetry in optics, *Phys. Scr.* **85**, 058101 (2012).

[23] S. A. Aljunid, G. Maslennikov, Y. Wang, H. L. Dao, V. Scarani, and C. Kurtsiefer, Excitation of a Single Atom with Exponentially Rising Light Pulses, *Phys. Rev. Lett.* **111**, 103001 (2013).

[24] S. Ritter, C. Nölleke, C. Hahn, A. Reiserer, A. Neuzner, M. Uphoff, M. Mücke, E. Figueroa, J. Bochmann, and G. Rempe, An elementary quantum network of single atoms in optical cavities, *Nature* **484**, 195 (2012).

[25] A. Reiserer and G. Rempe, Cavity-based quantum networks with single atoms and optical photons, *Rev. Mod. Phys.* **87**, 1379 (2015).

[26] G. F. Peñas, R. Puebla, and J. José García-Ripoll, Improving quantum state transfer: correcting non-Markovian and distortion effects, *Quantum Sci. Technol.* **8**, 045026 (2023).

[27] K. Randles and S. J. van Enk, Quantum state transfer and input-output theory with time reversal, *Phys. Rev. A* **108**, 012421 (2023).

[28] G. F. Peñas, R. Puebla, and J. J. García-Ripoll, Multiplexed quantum state transfer in waveguides, *Phys. Rev. Res.* **6**, 033294 (2024).

[29] H. Thyrrstrup, A. Hartsuiker, J.-M. Gérard, and W. L. Vos, Non-exponential spontaneous emission dynamics for emitters in a time-dependent optical cavity, *Opt. Express*, *OE* **21**, 23130 (2013).

[30] W. Li, X. Dong, G. Zhang, and R.-B. Wu, Flying-qubit control via a three-level atom with tunable waveguide couplings, *Phys. Rev. B* **106**, 134305 (2022).

[31] M. R. Hush, C. D. B. Bentley, R. L. Ahlefeldt, M. R. James, M. J. Sellars, and V. Ugrinovskii, Quantum state transfer through time reversal of an optical channel, *Phys. Rev. A* **94**, 062302 (2016).

[32] J. Donohue, M. Mastrovich, and K. Resch, Spectrally Engineering Photonic Entanglement with a Time Lens, *Phys. Rev. Lett.* **117**, 243602 (2016).

[33] M. Karpiński, M. Jachura, L. J. Wright, and B. J. Smith, Bandwidth manipulation of quantum light by an electro-optic time lens, *Nature Photon* **11**, 53 (2017).

[34] M. G. Raymer, D. V. Reddy, S. J. van Enk, and C. J. McKinstrie, Time reversal of arbitrary photonic temporal modes via nonlinear optical frequency conversion, *New J. Phys.* **20**, 053027 (2018).

[35] P. Lodahl, S. Mahmoodian, and S. Stobbe, Interfacing single photons and single quantum dots with photonic nanostructures, *Rev. Mod. Phys.* **87**, 347 (2015).

[36] X. Gu, A. F. Kockum, A. Miranowicz, Y.-x. Liu, and F. Nori, Microwave photonics with superconducting quantum circuits, *Physics Reports Microwave photonics with superconducting quantum circuits*, **718-719**, 1 (2017).

[37] D. E. Chang, A. S. Sørensen, P. R. Hemmer, and M. D. Lukin, Quantum Optics with Surface Plasmons, *Phys. Rev. Lett.* **97**, 053002 (2006).

[38] A. Gonzalez-Tudela, D. Martin-Cano, E. Moreno, L. Martin-Moreno, C. Tejedor, and F. J. Garcia-Vidal, Entanglement of Two Qubits Mediated by One-Dimensional Plasmonic Waveguides, *Phys. Rev. Lett.* **106**, 020501 (2011).

[39] A. González-Tudela, C.-L. Hung, D. E. Chang, J. I. Cirac, and H. J. Kimble, Subwavelength vacuum lattices and atom-atom interactions in two-dimensional photonic crystals, *Nature Photon* **9**, 320 (2015).

[40] H. Pichler, T. Ramos, A. J. Daley, and P. Zoller, Quantum optics of chiral spin networks, *Phys. Rev. A* **91**, 042116 (2015).

[41] C. Gonzalez-Ballester, A. Gonzalez-Tudela, F. J. Garcia-Vidal, and E. Moreno, Chiral route to spontaneous entanglement generation, *Phys. Rev. B* **92**, 155304 (2015).

[42] M. Maffei, D. Pomarico, P. Facchi, G. Magnifico, S. Pascazio, and F. V. Pepe, Directional emission and photon bunching from a qubit pair in waveguide, *Phys. Rev. Res.* **6**, L032017 (2024).

[43] V. Weisskopf and E. Wigner, Berechnung der natürlichen Linienbreite auf Grund der Diracschenglisch Lichttheorie, *Z. Physik* **63**, 54 (1930).

[44] V. Weisskopf and E. Wigner, Über die natürliche Linienbreite in der Strahlung des harmonischen Oszillators, *Z. Physik* **65**, 18 (1930).

[45] R. M. Errico, What Is an Adjoint Model?, *Bulletin of the American Meteorological Society* **78**, 2577 (1997).

[46] Y. Cao, S. Li, L. Petzold, and R. Serban, Adjoint Sensitivity Analysis for Differential-Algebraic Equations: The Adjoint DAE System and Its Numerical Solution, *SIAM J. Sci. Comput.* **24**, 1076 (2003).

[47] S. G. Johnson, Notes on adjoint methods for 18.335, *Introduction to Numerical Methods* (2012).

[48] T. Li, A. Miranowicz, X. Hu, K. Xia, and F. Nori, Quantum memory and gates using a Lambda-type quantum emitter coupled to a chiral waveguide, *Phys. Rev. A* **97**, 062318 (2018).

[49] Z.-L. Zhang and L.-P. Yang, Limits of single-photon storage in a single Lambda-type atom, *Phys. Rev. A* **107**, 063704 (2023).

[50] T. Lund-Hansen, S. Stobbe, B. Julsgaard, H. Thyrrstrup, T. Sünder, M. Kamp, A. Forchel, and P. Lodahl, Experimental Realization of Highly Efficient Broadband Coupling of Single Quantum Dots to a Photonic Crystal Waveguide, *Phys. Rev. Lett.* **101**, 113903 (2008).

[51] E. Vetsch, D. Reitz, G. Sagué, R. Schmidt, S. T. Dawkins, and A. Rauschenbeutel, Optical Interface Created by Laser-Cooled Atoms Trapped in the Evanescent Field Surrounding an Optical Nanofiber, *Phys. Rev. Lett.* **104**, 203603 (2010).

[52] R. Mitsch, C. Sayrin, B. Albrecht, P. Schneeweiss, and A. Rauschenbeutel, Quantum state-controlled directional spontaneous emission of photons into a nanophotonic waveguide, *Nat Commun* **5**, 5713 (2014).

[53] A. Goban, C.-L. Hung, S.-P. Yu, J. D. Hood, J. A. Muniz, J. H. Lee, M. J. Martin, A. C. McClung, K. S. Choi, D. E. Chang, O. Painter, and H. J. Kimble, Atom-light interactions in photonic crystals, *Nat Commun* **5**, 3808 (2014).

[54] M. Arcari, I. Söllner, A. Javadi, S. Lindskov Hansen, S. Mahmoodian, J. Liu, H. Thyrrstrup, E. Lee, J. Song, S. Stobbe, and P. Lodahl, Near-Unity Coupling Efficiency of a Quantum Emitter to a Photonic Crystal Waveguide, *Phys. Rev. Lett.* **113**, 093603 (2014).

[55] A. Yariv, Y. Xu, R. K. Lee, and A. Scherer, Coupled-resonator optical waveguide: a proposal and analysis, *Opt. Lett.*, *OL* **24**, 711 (1999).

[56] T. Ramos, B. Vermersch, P. Hauke, H. Pichler, and P. Zoller, Non-Markovian dynamics in chiral quantum networks with spins and photons, *Phys. Rev. A* **93**, 062104 (2016).

[57] M. Christandl, N. Datta, A. Ekert, and A. J. Landahl, Perfect State Transfer in Quantum Spin Networks, *Phys. Rev. Lett.* **92**, 187902 (2004).

[58] P. Karbach and J. Stolze, Spin chains as perfect quantum

state mirrors, Phys. Rev. A **72**, 030301 (2005).

[59] S. J. Masson and A. Asenjo-Garcia, Atomic-waveguide quantum electrodynamics, Phys. Rev. Res. **2**, 043213 (2020).

[60] R. Stainko and O. Sigmund, Tailoring dispersion properties of photonic crystal waveguides by topology optimization, Waves in Random and Complex Media **17**, 477 (2007).

[61] J. M. C. Boggio, D. Bodenmüller, T. Fremberg, R. Haynes, M. M. Roth, R. Eisermann, M. Lisker, L. Zimmermann, and M. Böhm, Dispersion engineered silicon nitride waveguides by geometrical and refractive-index optimization, J. Opt. Soc. Am. B, JOSAB **31**, 2846 (2014).

[62] D. Gray, G. N. West, and R. J. Ram, Inverse design for waveguide dispersion with a differentiable mode solver, Opt. Express, OE **32**, 30541 (2024).

[63] J.-T. Shen and S. Fan, Strongly Correlated Two-Photon Transport in a One-Dimensional Waveguide Coupled to a Two-Level System, Phys. Rev. Lett. **98**, 153003 (2007).

[64] J.-T. Shen and S. Fan, Strongly correlated multiparticle transport in one dimension through a quantum impurity, Phys. Rev. A **76**, 062709 (2007).

[65] B. Srivathsan, G. K. Gulati, A. Cerè, B. Chng, and C. Kurtsiefer, Reversing The Temporal Envelope Of A Heralded Single Photon Using A Cavity, in *2015 European Conference on Lasers and Electro-Optics - European Quantum Electronics Conference (2015)*, paper EA\_6\_2 (2015) p. EA\_6\_2.

[66] B. Kraus and J. I. Cirac, Discrete Entanglement Distribution with Squeezed Light, Phys. Rev. Lett. **92**, 013602 (2004).

[67] J. Agustí, X. Zhang, Y. Minoguchi, and P. Rabl, Autonomous Distribution of Programmable Multiqubit Entanglement in a Dual-Rail Quantum Network, Phys. Rev. Lett. **131**, 250801 (2023).

[68] A. Asenjo-Garcia, M. Moreno-Cardoner, A. Albrecht, H. Kimble, and D. Chang, Exponential Improvement in Photon Storage Fidelities Using Subradiance and “Selective Radiance” in Atomic Arrays, Phys. Rev. X **7**, 031024 (2017).

[69] R. Pennetta, M. Blaha, A. Johnson, D. Lechner, P. Schneeweiss, J. Volz, and A. Rauschenbeutel, Collective Radiative Dynamics of an Ensemble of Cold Atoms Coupled to an Optical Waveguide, Phys. Rev. Lett. **128**, 073601 (2022).

[70] S. Cardenas-Lopez, S. J. Masson, Z. Zager, and A. Asenjo-Garcia, Many-Body Superradiance and Dynamical Mirror Symmetry Breaking in Waveguide QED, Phys. Rev. Lett. **131**, 033605 (2023).

[71] C. Cohen-Tannoudji, J. Dupont-Roc, and G. Grynberg, eds., *Atom-photon interactions: basic processes and applications*, A Wiley-Interscience publication (Wiley, New York, NY, 2008).

[72] A. González-Tudela and J. I. Cirac, Markovian and non-Markovian dynamics of quantum emitters coupled to two-dimensional structured reservoirs, Phys. Rev. A **96**, 043811 (2017).

[73] P. Yeh, *Optical Waves in Layered Media* (Wiley, New York, 1988) chap. 8.

## END MATTER

## Resolvent solution to nonlinear dispersion

The dynamics of a single qubit coupled to a dispersion-engineered waveguide can be solved using the resolvent method [71, 72]. To this end, we calculate the self-energy,

$$\begin{aligned}\Sigma(\Delta + i0^+) &= g^2 \int dk \frac{1}{\delta - \delta(k) + i0^+} \\ &= -\frac{i\pi g^2}{d} \left[ \Delta t + \frac{2}{i\delta - \gamma} \right],\end{aligned}\quad (6)$$

where  $\Delta t$  is the time until absorption,  $\delta \equiv \omega - \omega_q$  and  $\delta(k) \equiv \omega(k) - \omega_q$ . To derive the above expression, we substitute  $d\delta = k'(\delta) dk$  and, exploiting that  $k'(\delta)$  is meromorphic [see Eq. (3)], employ the Sokhotski–Plemelj and residue theorem. We use this self-energy to describe the exact dynamics of the initially excited first qubit,

$$c_1(t) = e^{-i\omega_q t} \frac{i}{2\pi} \int_{-\infty}^{\infty} d\delta \frac{e^{-i\delta t}}{\delta - \Sigma(\delta + i0^+)}, \quad (7)$$

which can again be solved using the residue theorem. For the integrand we find poles at  $\delta_0 = i\gamma$ ,  $\delta_{1,2} = -i\gamma_{1,2}$ , which yields the expressions of Eq. (4) in the main text upon closing the contour in the lower half plane.

From the qubit dynamics in the nonlinear dispersion, we can derive the corresponding solution for the emitted pulse,

$$c(k; t) = -g \sum_{i=1}^2 w_i \frac{e^{-(\gamma_i + i\omega_q)t} - e^{-i(\delta(k) + \omega_q)t}}{\delta(k) + i\gamma_i}, \quad (8)$$

which upon Fourier transforming with respect to  $k$  and  $t$  yields

$$\begin{aligned}c(x_1, \delta) &= g \sum_{i=1}^2 w_i \left[ \frac{1}{\delta + i\gamma_i} \frac{1}{v_g} \left( 1 + \frac{2v_g}{d\gamma} \right) \right. \\ &\quad \left. - \frac{i}{d} \frac{1}{(\delta + i\gamma_i)(\delta + i\gamma)} \right].\end{aligned}\quad (9)$$

We can now use this expression to derive a corrected dispersion relation in analogy to the derivation in the main text. Equation (3) can be rewritten for arbitrary pulse shapes,

$$k(\omega) = \frac{\Delta t}{d} \omega - \frac{2}{d} \arg[c(x_1, \delta)]. \quad (10)$$

Inserting Eq. (9), we find that the resulting  $k(\omega)$  is not uniquely invertible, i.e., it cannot be implemented using a single band for  $d \lesssim 1.7v_g/\gamma$ . While a multi-band dispersion is not fundamentally impossible to engineer, our iterative process, which assumes a single band, halts here.

## Optimizing dispersion for close qubits

To optimize the dispersion relation we use a gradient descent approach. We efficiently determine the gradient by an adjoint method. In the following, we work with a discretized formulation of the wavefunction [see Eq. (2)], as is necessary for calculating the dynamics using exact diagonalization. The photonic amplitudes  $c(k, t)$  are discretized on  $N$  momenta  $k_1, \dots, k_N$  which are spaced equidistantly with spacing  $\Delta k$  such that the wavefunction is a complex vector of dimension  $N + 2$ ,

$$\psi = \sum_{i=1}^2 c_i(t) \mathbf{e}_i + \sum_{i=3}^{N+2} \sqrt{\Delta k} c(k_{i-2}, t) \mathbf{e}_i, \quad (11)$$

where  $\mathbf{e}_i$  are standard cartesian basis vectors and a rescaling by  $\sqrt{\Delta k}$  is necessary to take  $\psi$  to be normalized in the euclidean sense. At the same time, also the coupling constants in the discrete approximation are scaled by  $\sqrt{\Delta k}$  to account for a constant density of states. The cost function for the excitation transfer is

$$\mathcal{G}(\mathbf{p}, \psi) = \psi^\dagger P_2 \psi, \quad (12)$$

with  $P_2 = \mathbf{e}_2 \mathbf{e}_2^\dagger$  the projector on the state where only the second qubit is excited. We denote the parameters to be optimized by  $\mathbf{p} = (\Delta t, \omega_1, \dots, \omega_N)$ . Here,  $\Delta t$  is the time where we evaluate  $\psi$  in the dynamics, i.e., the time of maximal absorption, and the dispersion relation was discretized on  $N$  equidistant points corresponding to the discretization in  $k$ -space. The dependence of the cost function on  $\mathbf{p}$  is only implicit via  $\psi$ , such that we can write the gradient as

$$\nabla \mathcal{G} = \frac{\partial \mathcal{G}}{\partial \psi} \frac{\partial \psi}{\partial \mathbf{p}} + \frac{\partial \mathcal{G}}{\partial \psi^*} \frac{\partial \psi^*}{\partial \mathbf{p}} = 2 \operatorname{Re}(\mathcal{G}_\psi \psi_\mathbf{p}), \quad (13)$$

where we use the notation  $(\psi_\mathbf{p})_i = \partial_{p_i} \psi$ . Following Ref. [47] we can write the gradient as

$$\nabla \mathcal{G} = -2 \operatorname{Re}(g_\psi A^{-1} A_\mathbf{p} \psi) = -2 \operatorname{Re}(\psi^\dagger P_2 A^\dagger A_\mathbf{p} \psi), \quad (14)$$

where  $A$  is the inverse time evolution operator and  $(A_\mathbf{p})_i = \partial_{p_i} A$ . We can directly evaluate the derivative with respect to the evaluation time,

$$\frac{\partial \mathcal{G}}{\partial \Delta t} = 2 \operatorname{Im}(\psi^\dagger P_2 H \psi), \quad (15)$$

where  $H$  is the discretized pendant of Eq. (1). For the derivative with respect to  $\omega_i$ , the derivative of the time evolution operator leads to an integral

$$A_{\omega_i} = i \int_0^t dt' e^{iHt'} H_{\omega_i} e^{iH(t-t')}, \quad (16)$$

where  $H_{\omega_i} = \mathbf{e}_{i+2} \mathbf{e}_{i+2}^\dagger$  projects on the basis state corresponding to discretized frequency  $\omega_i$ . Since we work with

exact diagonalization to calculate the dynamics, we can explicitly evaluate the integral in terms of eigenvalues  $E_l$  and eigenvectors  $v_l$  of the Hamiltonian, with  $U = (v_1, \dots, v_{N+2})$ ,  $D = \text{diag}(E_1, \dots, E_{N+2})$  and  $D = U^\dagger \mathcal{H} U$  and finally write

$$\frac{\partial \mathcal{G}}{\partial \omega_i} = 2\text{Im} \left[ \psi^\dagger(0) U e^{-iDt} U^\dagger e_2 \sum_{lm} e_2^\dagger U v_l e^{-iE_l t} \times v_l U^\dagger v_i v_i^\dagger U v_m C_{lm} \right], \quad (17)$$

where

$$C_{lm} = \begin{cases} t, & l = m, \\ \frac{e^{-iE_m t} - e^{-iE_l t}}{i(E_l - E_m)}, & l \neq m. \end{cases} \quad (18)$$

### Solution of a linear ramp

In this section, we derive the transmission and reflection coefficients of the linear ramp in Fig. 3(b). For convenience, we separate the dispersion  $k(\omega)$  into a non-dispersive part  $k_l(\omega)$  and a dispersive part  $k_d(\omega)$ :

$$k(\omega, x) = \begin{cases} k_l(\omega), & \text{if } |x| \geq L, \\ k_l(\omega) + k_d(\omega)(1 - |x|/L), & \text{if } |x| \leq L. \end{cases} \quad (19)$$

The non-dispersive part  $k_l(\omega) = \omega/v_g$  determines the arrival time of the pulse; the dispersive part  $k_d(\omega)$  is given by the nonlinear phase shift required to transform an exponentially increasing pulse into an exponentially decreasing one, which we have calculated in Eq. (3) to be  $\Delta\phi(\omega) = -2 \arctan[(\omega - \omega_q)/\gamma]$ . Integrating  $k_d(\omega)(1 - |x|/L)$  over the region  $x \in [-L, L]$  to match this phase, we obtain  $k_d(\omega) = \Delta\phi(\omega)/L$ . This dispersion relation ensures the right pulse transformation.

We seek a solution of wave propagating in the linear ramp of Eq. (19). The key equation to solve is the wave equation

$$\frac{d^2}{dx^2} E(x) + k^2(x) E(x) = 0, \quad (20)$$

where for simplicity we drop the  $\omega$  argument and assume everything implicitly depends on  $\omega$ . The solution of Eq. (20) can be analytically derived. For this, we follow Ref. [73], which shows fields in a monotonic linear ramp (i.e., either  $x \in [-L, 0]$  or  $x \in [0, L]$ ) can be expanded as  $E(x) = b_1 J(x) + b_2 Y(x)$  where  $J(x) = \sqrt{k(x)} J_{1/4}\left(\frac{k^2(x)}{2\alpha}\right)$ ,  $Y(x) = \sqrt{k(x)} Y_{1/4}\left(\frac{k^2(x)}{2\alpha}\right)$  and  $\alpha = k_d/L$ . Here,  $J_{1/4}(x)$  and  $Y_{1/4}(x)$  are Bessel functions of the first and second kinds, respectively. From

this, we can make the following ansatz for Eq. (20):

$$E(x) = \begin{cases} b_5 e^{ik_l x} + b_6 e^{-ik_l x}, & x < -L, \\ b_1 J(x) + b_2 Y(x), & -L < x < 0, \\ b_3 J(x) + b_4 Y(x), & 0 < x < L, \\ b_7 e^{ik_l x}, & L < x. \end{cases} \quad (21)$$

We solve the unknown coefficients by matching boundary conditions. We then calculate the reflection and transmission coefficients:  $r = b_6 e^{ik_l L} / (b_5 e^{-ik_l L})$  and  $t = b_7 e^{ik_l L} / (b_5 e^{-ik_l L})$ . The general expressions of  $r$  and  $t$  are too complicated to present here. We only show their asymptotes when  $L \gg \lambda = 2\pi v_g/\omega$ :

$$r(\omega) = \frac{ie^{i(k_l + k_s)L} k_d [k_l^2 - k_s^2 \cos(L(k_l + k_s))]}{2L k_l^2 k_s^2}, \quad (22)$$

$$t(\omega) = e^{i(k_l + k_s)L}, \quad (23)$$

where  $k_s = k_l + k_d$ . In this limit, the spatial variation of our dispersion  $k(x)$  satisfies the adiabatic condition  $|dk(x)/dx| \ll |k(x)|^2$ , under which the transmission  $t(\omega)$  is guaranteed to be unitary and accumulates a phase that is proportional to the optical thickness [73], which is also what we see in Eq. (23). As for the reflection, since  $k_d = \Delta\phi(\omega)/L$ , we can bound it by

$$R(\omega) = |r(\omega)|^2 \leq \frac{[\Delta\Phi(\omega)]^2}{L^4 k_l^4} \quad (24)$$

which shows a  $1/L^4$  dependence, guaranteeing near-unity transmission for long enough  $L$ . We plot  $R(\omega)$  for three frequencies in Fig. 3(c) and show they all decay to zero in the limit of  $L \gg \lambda_q$ .

We model the quantum dynamics by employing the Hamiltonian for the qubits located outside the inhomogeneous region,

$$\begin{aligned} H = & \omega_q \sum_{i=1}^2 \sigma_i^+ \sigma_i^- + \int_0^\infty dk \, ck \left( a_{Rk}^\dagger a_{Rk} + a_{Lk}^\dagger a_{Lk} \right) \\ & + g \int dk \left( e^{ikx_1} \sigma_1^\dagger a_{Rk} + \text{H.c.} \right) \\ & + g \int dk \left( b_7 e^{ikx_2} \sigma_2^\dagger a_{Rk} + b_6 e^{ikx_2} \sigma_2^\dagger a_{Lk} + \text{H.c.} \right). \end{aligned} \quad (25)$$

Here,  $a_{Rk}$  and  $a_{Lk}$  denote modes that correspond to the right and left propagating modes in a system without any back reflection, respectively. In the presence of an inhomogeneity, also the left propagating eigenmode has a right propagating contribution that couples to the second qubit.